Multivariate Pattern-Driven Regime Identification for Decision Support in Ti-6Al-4V Dry Machining

Wagner da Silva Moraes (PUC-Campinas) wagnermoraes_sjc@hotmail.com
Alex Fernandes de Souza (Universidade Federal de Itajubá) alex_fernandes1989@live.com

Abstract

This study identifies decision-support machining regimes for Ti-6Al-4V dry machining using a multivariate pattern-driven approach. The objective is to transform a large experimental dataset into actionable insights. Each regime is linked to distinct industrial strategies based on surface quality, cutting forces, and process robustness. The methodology starts with data preprocessing and feature enrichment. Dimensionality reduction is performed using PCA. Operational regimes are then identified through Ward hierarchical clustering in the principal component space. Statistical validation is conducted using MANOVA, while LDA is applied to assess geometric separation among regimes. Nonlinear relationships are explored with t-SNE, and categorical information is integrated using MCA. The results indicate that surface roughness shows weak global linear relationships. However, a clear regime structure emerges in the multivariate space. Three statistically distinct operational patterns are identified, each associated with specific parameter windows and stability profiles captured by compactness and coefficients of variation. In conclusion, the proposed regime-based framework offers a more interpretable and robust alternative to global optimization models. It enables practical decision rules for selecting cutting conditions aligned with finishing, productivity, and process stability objectives.

Keywords: Ti-6Al-4V, Dry Machining, Surface Roughness, Clustering, Multi-objective Optimization.

1. Introduction

The Ti-6Al-4V titanium alloy is widely used in aerospace, biomedical, and high-performance industrial applications due to its high specific strength, corrosion resistance, and biocompatibility. However, these same properties make its machining particularly challenging, especially under dry cutting conditions, where the absence of cutting fluids intensifies thermal effects, tool wear, and process instabilities. As a result, achieving surface quality, operational stability, and productivity simultaneously remains a critical challenge in manufacturing this material.

Most studies on Ti-6Al-4V machining rely on univariate or bivariate analyses, relating cutting parameters such as cutting speed and feed rate to individual process responses. Although informative, these approaches are limited when applied to highly nonlinear and multi-mechanistic processes. In particular, surface roughness often exhibits weak linear correlations with isolated variables, which hinders accurate prediction and optimization using conventional global models.

In this context, data-driven multivariate approaches have emerged as promising alternatives for analyzing complex machining processes. Techniques such as dimensionality reduction, unsupervised clustering, and low-dimensional projections enable the identification of latent patterns and distinct operational regimes in which the process exhibits relatively homogeneous behavior. This regime-based perspective shifts the focus from searching for a single global optimum to identifying consistent operating windows aligned with different industrial objectives.

The identification of machining regimes also provides practical advantages from a decision-making standpoint. Rather than relying exclusively on global predictive models, which are often sensitive to noise and extrapolation, regime-based analysis enables the definition of robust and interpretable operating ranges. This approach facilitates the association of each regime with specific industrial goals, such as surface finishing, productivity, or process stability, while supporting the integration of both quantitative and qualitative variables within a unified analytical framework.

Within this context, the objective of this study is to identify and characterize dry machining operational regimes of Ti-6Al-4V based on multivariate experimental data, using dimensionality reduction, unsupervised clustering, and multivariate statistical analysis. The aim is to transform a large and heterogeneous experimental dataset into decision-oriented information, associating each regime with distinct industrial strategies based on surface quality, cutting forces, process variability, and operational robustness.

2. Theoretical Background

Dry machining of Ti-6Al-4V generates multivariate datasets characterized by strong heterogeneity, partial correlations, and regime-dependent behavior. Experimental evidence shows that cutting forces, surface quality, and process stability emerge from nonlinear interactions that are not adequately described by global linear models, especially under dry cutting conditions (Siju et al., 2022; Klippel et al., 2024).

From a statistical perspective, the machining process can be represented as a multivariate system in which the response vector r results from an unknown nonlinear mapping of the process parameters v, corrupted by correlated noise:

$$r = f(v) + \varepsilon, \qquad \varepsilon \sim N(0, \Sigma)$$

(1)

Where Σ denotes the covariance structure of the process noise. This formulation highlights that relevant information is distributed across multiple correlated variables, making univariate analysis insufficient for reliable interpretation (Childerhouse et al., 2024).

The total variance of the multivariate response can be decomposed into within-regime and between-regime components, which explains why weak global correlations may coexist with strong local structures:

$$\mathrm{Var}(r) = \sum_k \mathrm{Var}(r \mid R_k)\, P(R_k) + \sum_k [E(r \mid R_k) - E(r)]^2\, P(R_k)$$

(2)

Where R_k represents statistically distinct operational regimes. This variance decomposition motivates regime-based analysis instead of global optimization approaches (Yadav and Yadav, 2020).

Principal Component Analysis (PCA) provides a formal statistical framework to extract latent structures from multivariate machining data. Given a normalized data matrix X with n observations and p variables, the covariance matrix is defined as:

$$\Sigma = (1 / (n - 1))\, X^T X$$

(3)

Where Σ captures the correlation structure among variables. The eigenvalue decomposition of Σ yields orthogonal directions that maximize variance, allowing dimensionality reduction without loss of dominant information (Greenacre et al., 2022).

The transformation into the principal component space is given by:

$$Z = XW \tag{4}$$

Where W is the matrix of eigenvectors associated with the largest eigenvalues of the covariance matrix. This linear transformation projects the original correlated variables into an orthogonal space, concentrating the dominant variance directions and reducing redundancy. As a result, the principal component scores Z provide a compact and informative representation of the machining process dynamics.

$$R^{2(m)} = \frac{\sum_{i=1}^{m} \lambda_i}{\sum_{j=1}^{p} \lambda_j} \tag{5}$$

Where λ_i are the eigenvalues of Σ. In machining applications, a small number of components typically captures most of the process variability, enabling effective regime identification (Amaral et al., 2023).

Once projected into the reduced space, clustering techniques allow the identification of statistically coherent regimes. The internal dispersion of each regime is quantified using its covariance structure, providing a measure of multivariate compactness that is directly linked to regime stability and interpretability.

Relative variability of key responses is evaluated using the coefficient of variation:

$$CV = \sigma / \mu \tag{6}$$

Where σ and μ represent the standard deviation and the mean of the response variable, respectively. This dimensionless metric normalizes dispersion by the central tendency, allowing consistent comparison of process stability across different machining regimes, even when the responses exhibit distinct magnitudes or scales (Sala et al., 2025).

Statistical separation among regimes is validated using Multivariate Analysis of Variance (MANOVA), which tests the null hypothesis of equality among group mean vectors in the joint variable space. The method relies on within-group and between-group scatter matrices to assess multivariate differences (Greenacre et al., 2022).

Linear Discriminant Analysis (LDA) complements MANOVA by projecting observations onto directions that maximize the ratio between inter-group and intra-group variance. The discriminant vectors are obtained by solving:

$$\mathrm{B\,w} = \lambda\,\mathrm{W\,w} \tag{7}$$

Where B and W denote the between-group and within-group scatter matrices. The resulting discriminant space provides a geometric interpretation of regime separation.

To integrate categorical process information, such as tool wear states, Multiple Correspondence Analysis (MCA) is employed. MCA supports joint interpretation of qualitative states and statistically identified regimes, strengthening the link between regime structure and operational meaning (Souza et al., 2026).

Regime-level decision support is achieved by combining multivariate compactness and variability metrics into a composite decision score. This strategy prioritizes robustness and statistical consistency over isolated optimal points, aligning the analytical framework with data-driven decision-making approaches used across Ti-6Al-4V-related studies (Alfred and Amiri, 2025; Yu et al., 2025; Li et al., 2024; Awd and Walther, 2025).

3. Methodology

The experimental data used in this study were obtained from the large-scale dry orthogonal cutting experiments conducted by Klippel et al. (2024) on Ti-6Al-4V alloy. The material, containing 6 wt.% aluminum and 4 wt.% vanadium with α (hcp) and β (bcc) phases, was machined as thin-walled cylindrical specimens (72 mm diameter and 2 mm wall thickness) using a Schaublin 42 L CNC lathe. A fractional factorial design was employed, comprising 26 cutting speed levels (10–500 m/min) and 11 feed levels (0.01–0.40 mm/rev), resulting in 109 parameter combinations and 287 experimental trials with 2–3 replications. The depth of cut was kept constant under quasi-orthogonal cutting conditions. Cutting forces were measured using a Kistler 9121A5 dynamometer, filtered at 30 Hz and sampled at 1.1 kHz, with analysis focused on the main cutting force component (Fc). Tool wear of Sandvik Coromant CCMW 09T304 H13A inserts was qualitatively classified as Low (L), Medium (M), or High (H).

The proposed analytical methodology followed a six-step workflow aimed at transforming heterogeneous experimental data into decision-oriented insights. First, data preprocessing and enrichment were performed, including numerical encoding of categorical variables, treatment of missing values, and construction of physically meaningful derived metrics. These included specific cutting energy (Fc/(vc·f)), force ratio (Ff/Fc), and material removal rate (MRR = vc·f), increasing the explanatory power of the dataset without introducing new experimental variables.

In the second step, Principal Component Analysis (PCA) was applied after standard normalization to reduce dimensionality and identify latent multivariate structures. PCA enabled the identification of dominant patterns governing surface roughness and cutting forces, which are not captured by conventional bivariate analyses.

The third step focused on regime identification using agglomerative hierarchical clustering with Ward’s method, applied to the first three principal components. The optimal number of clusters was defined through dendrogram inspection and the elbow criterion. Linear Discriminant Analysis (LDA) was subsequently used to assess cluster separability and classification robustness.

In the fourth step, nonlinear visualization techniques were incorporated to support interpretation. t-SNE was used to project observations into a two-dimensional space, highlighting local similarities and cluster coherence. Multiple Correspondence Analysis (MCA) was additionally employed to integrate categorical variables, such as tool wear and trial status, into the multivariate framework.

The fifth step consisted of multivariate cluster characterization. For each regime, compactness metrics, coefficients of variation of surface roughness (Ra) and cutting force (Fc), operational success rates, and dominant variable contributions were evaluated using PCA loadings and descriptive statistics.

Finally, a decision-support framework was developed, translating the identified regimes into actionable recommendations. Comparative matrices, multivariate radar charts, and context-dependent decision rules were used to link each regime to specific industrial objectives, such as surface quality, productivity, or process robustness. All analyses were implemented in Python 3.9 using scikit-learn, SciPy, prince, and plotly, ensuring reproducibility and adaptability to other machining contexts. Figure 1 shows the methodological framework adopted for multivariate regime identification and decision support.

Figure 1 - Overview of the methodological framework adopted for multivariate analysis and regime identification.

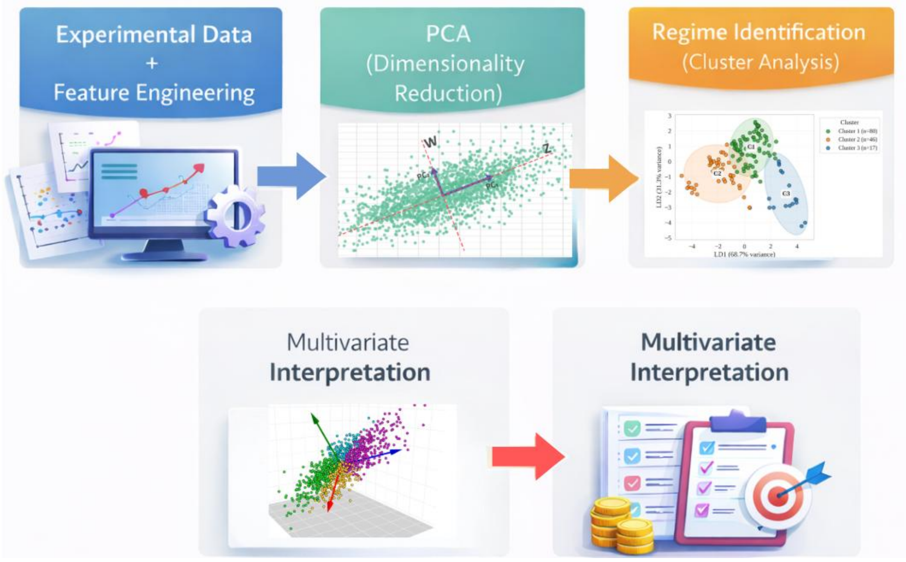

Source: Authors (2026).

The workflow starts from experimental data acquisition and feature engineering, followed by dimensionality reduction to extract latent multivariate structures. These structures are then used for regime identification and statistical validation, which are subsequently interpreted through multivariate visualization techniques. Finally, the identified regimes are synthesized into a decision-support framework, translating statistical patterns into practical operating guidelines for Ti-6Al-4V dry machining.

4. Results and Discussion

The analysis of linear relationships among the machining variables provides an initial understanding of how cutting parameters and process responses interact under dry machining conditions. Figure 2 presents the pairwise distributions and scatter plots of cutting speed, feed rate, cutting forces, and surface roughness, complemented by kernel density estimates along the diagonal. In parallel, the Pearson correlation matrix quantitatively summarizes these relationships, allowing the identification of dominant dependencies and weakly coupled variable **Fonte**: Autores (2026).

s that may require multivariate or regime-based interpretation.

Figure 2 - Pairwise Distributions of Machining Variables.

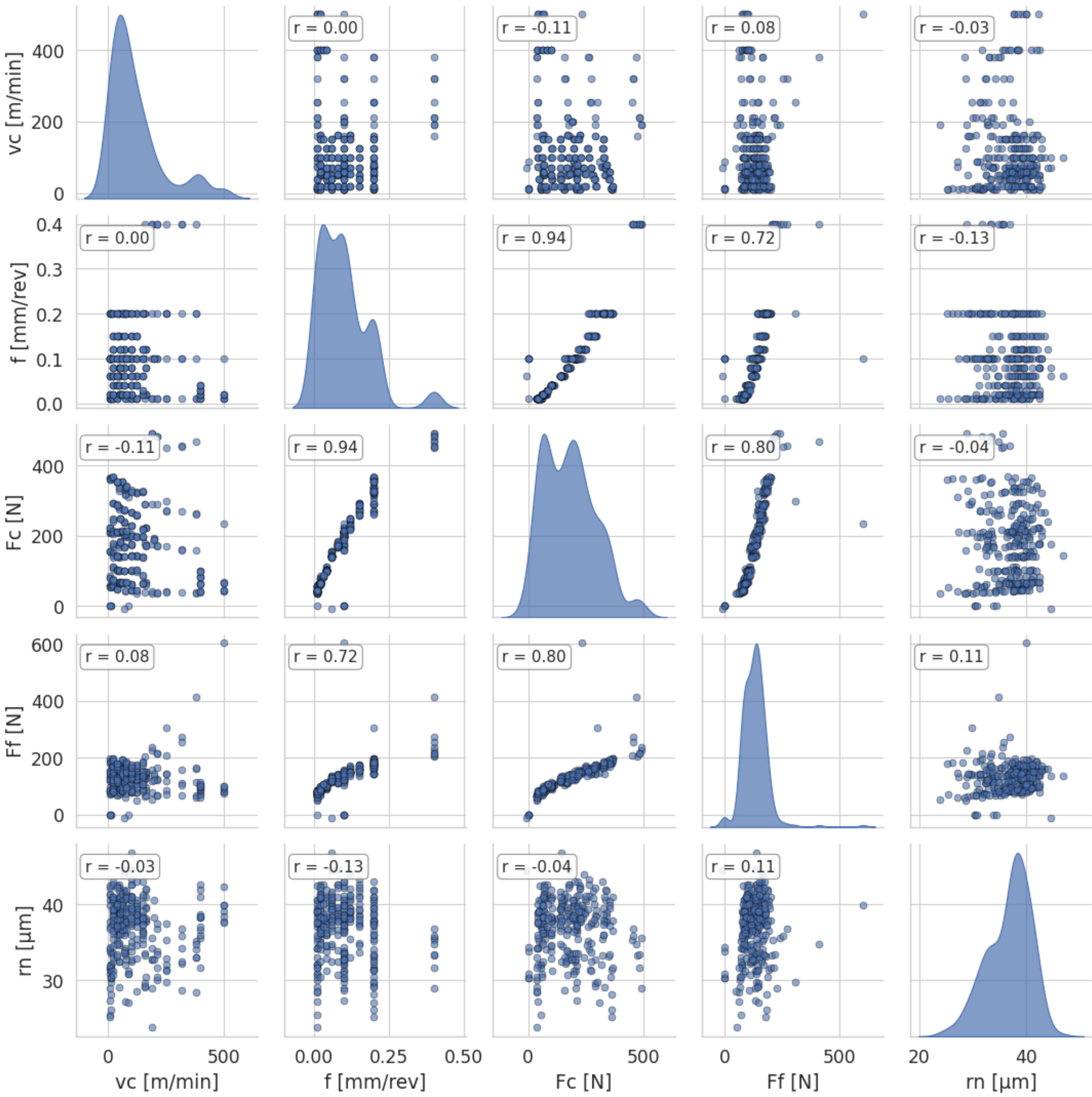

Source: Authors (2026).

As shown in Figure 2, strong linear correlations are observed between feed rate and cutting force (r = 0.94), as well as between feed rate and feed force (r = 0.72), confirming the expected mechanical relationship between chip load and force generation. A similarly strong correlation is observed between the cutting force components Fc and Ff (r = 0.80), indicating that both forces respond coherently to changes in material removal conditions. In contrast, cutting speed exhibits near-zero correlation with feed ($r = 0.00$) and only weak correlations with force components, suggesting that its influence on process mechanics is more indirect and potentially mediated by thermal or dynamic effects rather than purely mechanical loading.

Surface roughness (Ra) shows weak linear correlations with all primary cutting parameters and forces, with correlation coefficients ranging from −0.13 to 0.11. As illustrated in the lower row of Figure 1, the scatter plots involving rn display broad dispersion and overlapping distributions across the parameter space, indicating that surface roughness cannot be adequately explained by any single variable in isolation. This behavior highlights the limitation of global linear models for roughness prediction and reinforces the need for multivariate and regime-oriented approaches. The weak correlation between roughness and cutting forces, in particular, suggests that competing mechanisms—such as tool–material adhesion, built-up edge formation, and localized thermal effects, play a significant role in surface formation during dry machining of Ti-6Al-4V, masking simple linear trends.

Given the weak and diffuse linear relationships observed in the correlation analysis, an unsupervised multivariate approach was adopted to identify latent operational regimes within the experimental dataset. Figure 3 presents the hierarchical clustering structure obtained using Ward's method applied to the first three principal components, together with the elbow criterion used to support the selection of the number of clusters.

Figure 3 - Hierarchical clustering dendrogram and elbow criterion indicating three operational machining regimes.

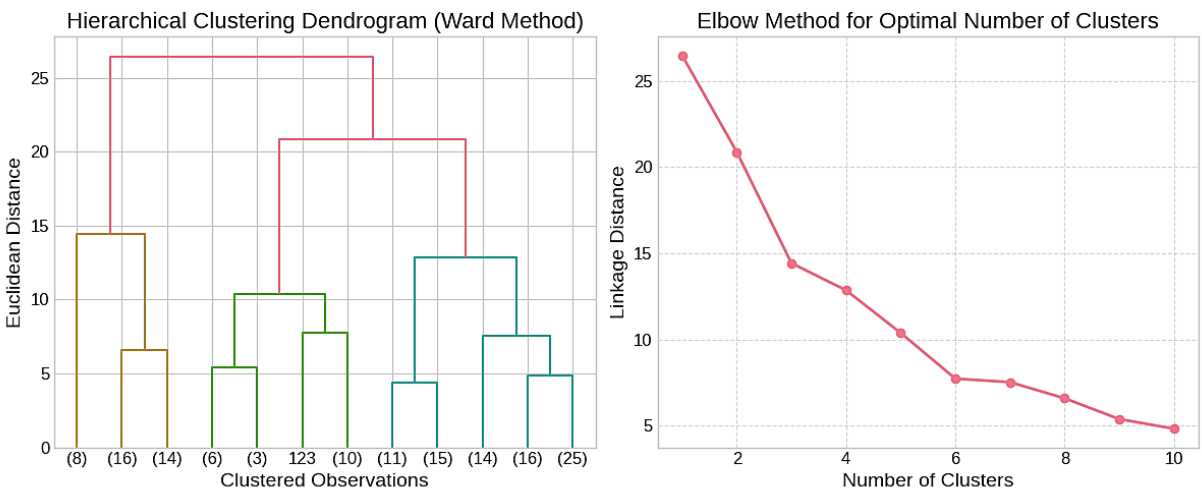

Source: Authors (2026).

As shown in Figure 3, the hierarchical dendrogram reveals clear separation among groups at relatively high linkage distances, indicating the presence of natural partitions in the multivariate space.

The elbow plot further supports the selection of three clusters, as a pronounced reduction in linkage distance is observed up to $k = 3$, followed by a more gradual decrease for higher values. This behavior suggests that three clusters capture the dominant structure of the data without over-fragmentation. These clusters therefore represent distinct machining regimes characterized by different combinations of cutting speed, feed rate, and force responses, providing a robust foundation for subsequent regime-specific analysis and decision-oriented interpretation.

To statistically validate the distinctiveness of the identified operational regimes, a one-way Multivariate Analysis of Variance (MANOVA) was conducted using the hierarchical cluster assignment as the grouping factor, as summarized in Table 1. The multivariate response vector comprised the main process outputs, including surface roughness and cutting force-related variables.

Table 1 - Multivariate analysis of variance (MANOVA) results for cluster effect.

Test statistic	Value	Num DF	Den DF	F value	p-value
Wilks' lambda	0.1041	10	264	55.41	< 0.001
Pillai's trace	1.3329	10	266	53.15	< 0.001
Hotelling–Lawley trace	4.4063	10	195.27	57.88	< 0.001
Roy's greatest root	3.0135	5	133	80.16	< 0.001

The MANOVA results revealed a highly significant cluster effect across all multivariate test statistics (Wilks' lambda, Pillai's trace, Hotelling–Lawley trace, and Roy's greatest root), with $p < 0.001$ in all cases. In particular, the low Wilks' lambda value (0.104) combined with the high Pillai's trace (1.333) indicates strong multivariate separation among the three clusters, confirming that the identified regimes differ substantially in their combined process responses.

Beyond statistical significance, the analysis demonstrates that regime separation emerges from the combined behavior of surface roughness and cutting force responses in the multivariate space. The consistent significance observed across all MANOVA test statistics confirms a stable and well-defined cluster structure, independent of the specific multivariate criterion adopted. As a result, the identified regimes correspond to meaningful and distinct operational behaviors rather than statistical artifacts, supporting their use in subsequent discriminant analysis and decision-oriented interpretation.

Figure 4 presents the projection of the experimental data onto the first two linear discriminant axes obtained by Linear Discriminant Analysis (LDA). This representation complements the MANOVA findings by offering a geometric interpretation of the statistically significant differences observed among the machining regimes. While MANOVA establishes the existence of multivariate differences, the LDA projection illustrates how these differences translate into clearly separable regions in a reduced-dimensional discriminant space, thereby enhancing interpretability.

Figure 4 - Linear Discriminant Analysis (LDA) projection of dry machining regimes in Ti-6Al-4V.

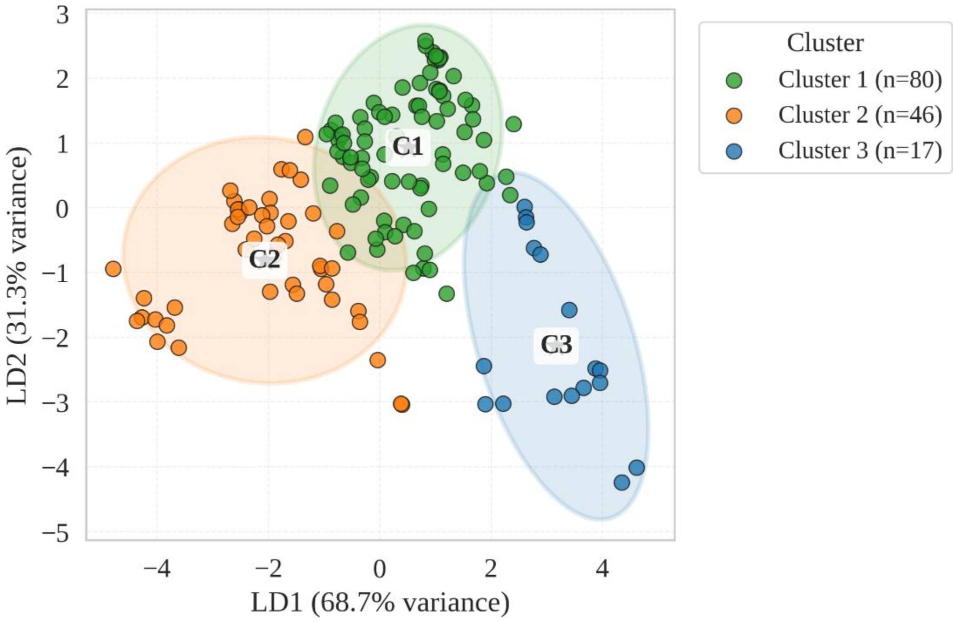

Source: Authors (2026).

As shown in Figure 4, the three machining regimes exhibit clear separation in the LDA space, with the first discriminant axis (LD1) accounting for 68.7% of the between-class variance and the second axis (LD2) explaining an additional 31.3%. Cluster 1 (green) occupies a compact and centrally located region, indicating relatively homogeneous operating conditions consistent with stable and conventional machining behavior. In contrast, Cluster 2 (orange) is shifted toward negative LD1 values and displays greater dispersion, suggesting increased variability associated with higher feed-driven strategies.

Cluster 3 (blue) is clearly isolated along both discriminant axes, reflecting a distinct regime characterized by extreme cutting conditions and reduced process stability. The limited overlap among the confidence ellipses further supports the robustness of the regime identification, reinforcing the conclusion that the observed clusters correspond to statistically and operationally distinct machining behaviors rather than artifacts of random variability.

To further explore the structure of these regimes beyond linear projections, Figure 5 presents a two-dimensional t-SNE embedding of the experimental dataset, highlighting the underlying nonlinear relationships among machining conditions. In the left panel, observations are colored according to cluster membership, revealing three well-defined regions in the reduced space, with cluster centroids indicated for reference. In the right panel, the same embedding is colored by surface roughness (Ra), allowing a direct visual assessment of how surface quality varies across the nonlinear manifold formed by the machining process.

Figure 5 - Nonlinear t-SNE visualization of machining regimes and surface roughness distribution.

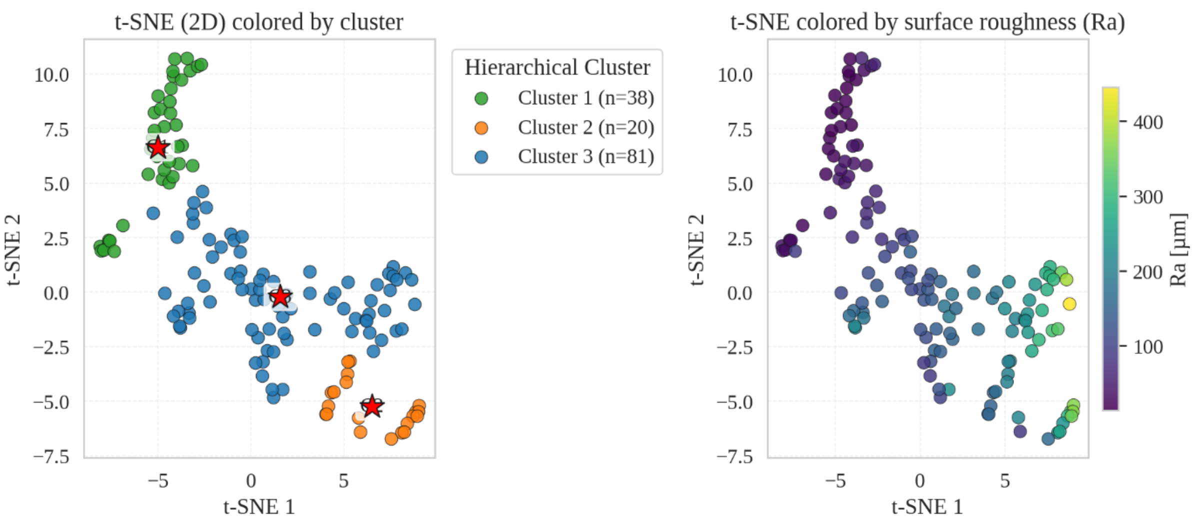

Source: Authors (2026).

From a discussion perspective, Figure 5 complements the previous MANOVA and LDA analyses by uncovering nonlinear relationships that are not fully captured by linear projections. The clear spatial separation among clusters reinforces the statistical evidence of regime distinctiveness, while the Ra-colored map reveals smooth gradients of surface roughness within and across clusters. In particular, clusters occupying distinct regions of the t-SNE space exhibit systematically different Ra levels, indicating that surface roughness is strongly regime-dependent and follows nonlinear patterns in the process parameter space. This visualization supports the interpretation that regime identification is not merely a clustering artifact but reflects meaningful underlying process dynamics, further justifying the use of regime-based decision support rather than global, one-size-fits-all optimization strategies.

Another analysis performed in this study was Multiple Correspondence Analysis (MCA), shown in Figure 6, aiming to investigate the associations between categorical process variables, specifically tool wear levels (Wear) and experimental process status (Status), in relation to the machining regimes identified by hierarchical clustering. Unlike the previously applied multivariate techniques, MCA is particularly suited for exploring co-occurrence patterns among qualitative variables, providing a complementary perspective on the operational consistency and semantic coherence of the identified regimes.

Figure 6 - Multiple Correspondence Analysis (MCA) map of tool wear and process status across machining regimes.

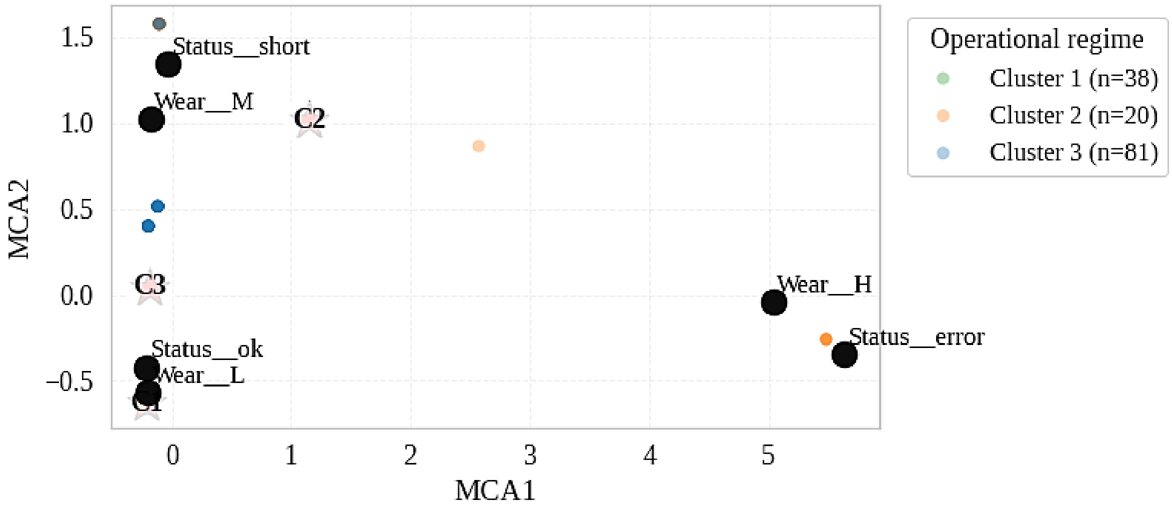

Source: Authors (2026).

The MCA projection reveals clear and meaningful associations between machining regimes and qualitative process outcomes. Cluster 3 is strongly associated with the categories Status_ok and Wear_L, characterizing a stable operational regime with low tool wear and high process reliability. In contrast, Cluster 2 shows close proximity to Status_error and Wear_H, indicating critical machining conditions marked by a high incidence of failures and severe tool degradation. Cluster 1 occupies an intermediate position in the MCA space, primarily associated with Wear_M and Status_short, suggesting a transitional regime in which machining remains feasible but with increased mechanical demand and reduced robustness. Overall, these findings reinforce the validity of the identified regimes by linking quantitative clustering results to qualitative operational states, thereby strengthening the decision-support capability of the proposed framework.

Following the identification and validation of the operational regimes through hierarchical clustering, MANOVA, and low-dimensional projections, the next step focused on a decision-oriented multivariate analysis aimed at characterizing the practical behavior of each regime. In this stage, the analysis emphasizes multivariate compactness and variability-related indicators, which are more informative for process stability and robustness than binary success metrics. The success rate was therefore retained only as a descriptive attribute and excluded from the decision score computation.

The multivariate characterization results appear in Table 2, detailing cluster size, multivariate compactness in PC space, coefficients of variation for surface roughness and cutting force, and the dominant operational pattern identified from PCA loadings and cluster centroids.

Table 2 - Raw multivariate metrics of the identified machining regimes.

Cluster	Size	Multivariate Compactness	Ra_CV	Force_CV	Dominant_Pattern
1	38	1.001	0.467	0.293	Low-Energy Pattern
2	20	0.678	0.368	0.281	High-Energy Pattern
3	81	1.021	0.470	0.362	Conservative Pattern

The results reveal clear structural differences among the identified regimes. Cluster 3 shows the highest multivariate compactness, indicating a conservative operating behavior with limited dispersion in the principal component space. This apparent stability, however, coexists with higher variability in cutting forces, suggesting that mechanical responses within this regime are not uniform.

By contrast, Cluster 2, identified as a high-energy pattern, presents the lowest compactness while simultaneously exhibiting the lowest coefficients of variation for both surface roughness and cutting forces. This combination points to a more consistent and predictable process response, even under aggressive operating conditions. Cluster 1 presents an intermediate behavior, combining moderate compactness with moderate variability levels, consistent with a low-energy operational pattern.

To support regime selection from a decision-making perspective, a composite decision score was computed based solely on multivariate compactness, surface roughness variability, and force variability. The success rate was excluded from the score calculation, as it did not contribute to cluster discrimination. The resulting normalized scores and overall ranking are presented in Table 3.

Table 3 - Decision scores and ranking based on multivariate stability criteria**.**

Cluster	Rank	Decision_Score	Multivariate_Compactness_score	Ra_CV_score	Force_CV_score
1	2	0.571	0.944	0.028	0.849
2	1	0.611	0.000	1.000	1.000
3	3	0.389	1.000	0.000	0.000

The ranking highlights Cluster 2 as the most favorable operational regime from a decision-oriented perspective. Despite its lower multivariate compactness, this regime achieves the highest overall score due to its superior stability in surface roughness and cutting force responses. Cluster 1 ranks second, benefiting from balanced compactness and moderate variability, while Cluster 3 ranks last, as its high compactness does not compensate for the elevated variability in key output variables. These results reinforce the importance of variability control over mere data concentration when evaluating machining regimes for practical deployment.

To further understand the distinctive dynamics of each regime, Figure 7 presents the Pearson correlation matrices computed separately for each hierarchical cluster. This regime-specific analysis reveals how relationships among cutting parameters (cutting speed and feed rate), surface roughness, and cutting force components vary across operational patterns. By examining correlations within rather than between clusters, the figure provides insight into how variable interdependencies evolve under different machining conditions, offering a nuanced view of the underlying process dynamics.

Figure 7 – Within-regime Pearson correlation structure of machining variables.

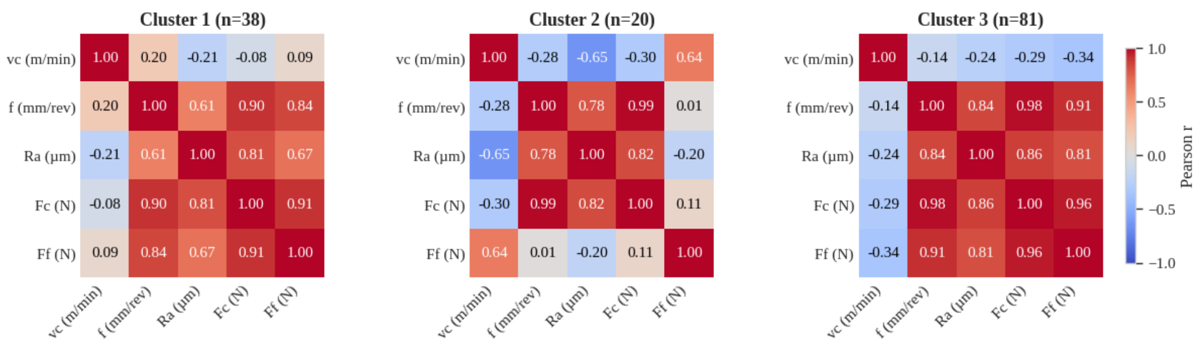

Source: Authors (2026).

The correlation structures reveal distinct behavioral signatures for each regime. Cluster 2 (high-energy pattern) exhibits very strong correlations between feed rate and cutting force components, as well as between surface roughness and cutting forces, indicating a tightly coupled mechanical response dominated by aggressive material removal conditions. In contrast, Cluster 1 (low-energy pattern) shows moderately strong but more balanced correlations, suggesting a smoother interaction between process parameters and output variables.

Cluster 3 (conservative pattern) is characterized by consistently high correlations among feed rate, surface roughness, and cutting forces, reflecting a stable yet force-sensitive regime. Overall, these results reinforce that each operational regime is governed by a distinct correlation structure, supporting the validity of the clustering approach and underscoring the importance of regime-dependent modeling and optimization strategies.

To support practical implementation, Table 4 consolidates the multivariate clustering results into a decision-oriented summary. This table links process parameter ranges, performance metrics, and internal variability for each machining regime, integrating cutting conditions (vc and f), output responses (Ra, Fc, and Ff), and multivariate compactness to characterize how each regime behaves in practice.

Table 4 - Decision-oriented summary of hierarchical machining regimes.

Cluster	n	vc range (m/min)	f range (mm/rev)	Ra mean ± std (µm)	Fc mean (N)	Ff mean (N)	Compactness	Ra CV	Force CV	Interpretation of regime
1	38	10–500	0.01–0.04	31.89 ± 14.90	54	81	1.001	0.467	0.293	Low-force, low-roughness regime with wide speed variability
2	20	159–500	0.10–0.40	223.71 ± 82.25	363	227	0.678	0.368	0.281	High-energy, high-load regime dominated by aggressive feeds
3	81	10–381	0.02–0.20	171.96 ± 80.82	223	144	1.021	0.470	0.362	Conservative regime with moderate forces and broad variability

Cluster 1 is characterized by low cutting forces and the lowest average surface roughness over a wide cutting speed range. Its high compactness and moderate coefficients of variation indicate stable and predictable behavior, making this regime suitable for finishing or semi-finishing operations where surface quality and process reliability are prioritized.

Cluster 2 represents a high-energy machining regime dominated by aggressive feed rates, resulting in the highest cutting forces and surface roughness levels. Despite its lower multivariate compactness, the relatively low variability of forces and roughness suggests consistent behavior, aligning this regime with roughing operations focused on productivity rather than surface quality.

Cluster 3 exhibits intermediate force and roughness levels combined with the highest multivariate compactness but elevated variability indicators. This behavior reflects a conservative, general-purpose regime that favors robustness across a broad range of conditions, trading optimized performance for increased tolerance to process fluctuations and operational uncertainty.

To operationalize these findings, Table 5 translates the multivariate analysis into a practical decision framework. By comparing real-time cutting conditions against the interquartile parameter windows of each cluster, practitioners can quickly identify the active machining regime without recomputing the full multivariate model.

Table 5 - Operational rules for rapid regime identification.

Cluster	vc typical window (Q1–Q3)	f typical window (Q1–Q3)	Fc typical window (Q1–Q3)	Operational rule
1	51–254	0.01–0.02	41–65	If current vc and f fall within this window, the process is likely operating in a low-energy, stable regime
2	190–318	0.20–0.40	271–469	Conditions within this window indicate a high-energy, aggressive machining regime
3	20–125	0.08–0.15	168–287	Parameters in this range suggest a conservative, robustness-oriented regime

This enables proactive adjustments, such as reducing feed when transitioning toward the high-energy regime or stabilizing cutting conditions to remain within conservative or low-energy windows, thereby supporting robust and informed decision-making in dry machining of Ti-6Al-4V.

5. Conclusion

The analysis conducted in this work highlights that the behavior of Ti-6Al-4V under dry machining cannot be adequately captured by single-response or globally optimized models. The observed dispersion in surface roughness and force responses indicates that multiple operational behaviors coexist within the same parameter space, which justifies the adoption of a multivariate, regime-oriented perspective.

The identification of statistically coherent machining regimes enabled the construction of practical decision rules based on stability and variability rather than isolated optimal points. This contributes to more reliable process planning by aligning cutting conditions with specific operational goals, reinforcing the value of regime-based analysis as a robust decision-support strategy for complex machining systems.

Acknowledgements

This study was financed in part by the Coordenação de Aperfeiçoamento de Pessoal de Nível Superior – Brasil (CAPES) – Finance Code 001

REFERENCES

ALFRED, Samuel Onimpa; AMIRI, Mehdi**.** A data-informed knowledge discovery framework to predict fatigue properties of additively manufactured Ti–6Al–4V, IN718 and AlSi10Mg alloys using fatigue databases. **Progress in Additive Manufacturing**, v. 10, n. [número se disponível], p. 6183-6210, set. 2025. Publicado online: 25 jan. 2025. Disponível em: https://doi.org/10.1007/s40964-025-00965-1. Acesso em: 14 jan. 2026.

AMARAL, Bruno Vitiello do; SOUZA, Alex Fernandes de; PETRUCCI, Ellen Rodrigues de Oliveira; MELLO, Carlos Henrique Pereira; CAMPOS, Paulo Henrique da Silva. Análise de componentes principais para variáveis do processo de torneamento a seco. In: **ENCONTRO NACIONAL DE ENGENHARIA DE PRODUÇÃO (ENEGEP)**, 43., 2023, Fortaleza. Anais… Rio de Janeiro: ABEPRO, 2023. Disponível em: https://doi.org/10.14488/enegep2023_tn_wpg_399_1956_46257. Acesso em: 13 jan. 2026.

AWD, Mustafa; WALTHER, Frank. AI-Powered Very-High-Cycle Fatigue Control: Optimizing Microstructural Design for Selective Laser Melted Ti-6Al-4V. **Materials**, v. 18, n. 7, 1472, 26 mar. 2025. Disponível em: https://doi.org/10.3390/ma18071472. Acesso em: 14 jan. 2026.

CHILDERHOUSE, Thomas et al**.** Rapid acquisition of digital fingerprints of Ti-6Al-4V macrotexture from machining force measurement data. **Materials Characterization**, v. 207, 113550, jan. 2024. Disponível em: https://doi.org/10.1016/j.matchar.2023.113550. Acesso em: 14 jan. 2026.

GREENACRE, Michael; GROENEN, Patrick J. F.; HASTIE, Trevor; D'ENZA, Alfonso Iodice; MARKOS, Angelos; TUZHILINA, Elena**.** Principal component analysis. **Nature Reviews Methods Primers**, v. 2, 100, 22 dez. 2022. Disponível em: https://doi.org/10.1038/s43586-022-00184-w. Acesso em: 14 jan. 2026.

KLIPPEL, Hagen; SÜSSMAIER, Stefan; ZHANG, Nanyuan; KUFFA, Michal; WEGENER, Konrad. Large-scale investigation of dry orthogonal cutting experiments Ti6Al4V and Ck45. **The International Journal of Advanced Manufacturing Technology,** London, v. 135, p. 2871–2908, 2024. Disponível em: https://doi.org/10.1007/s00170-024-14597-2. Acesso em: 13 jan. 2026.

LI, Gan; FAN, Qunbo; LI, Guoju; YANG, Lin; GONG, Haichao; LI, Meiqin; XU, Shun; CHENG, Xingwang. Unveiling the quantitative relationship between microstructural features and quasi-static tensile properties in dual-phase titanium alloys based on data-driven neural networks. **Materials Science and Engineering: A**, v. 913, 147102, out. 2024. Disponível em: https://doi.org/10.1016/j.msea.2024.147102. Acesso em: 14 jan. 2026.

SALA, Siva Teja; BOCK, Frederic E.; PÖLTL, Dominik; KLUSEMANN, Benjamin; HUBER, Norbert; KASHAEV, Nikolai. Deformation by design: data-driven approach to predict and modify deformation in thin Ti-6Al-4V sheets using laser peen forming. **Journal of Intelligent Manufacturing**, v. 36, n. 2, p. 639-659, jan. 2025. Disponível em: https://doi.org/10.1007/s10845-023-02240-y. Acesso em: 14 jan. 2026.

SIJU, Amal S.; JOSE, Sandeep; WAIGAONKAR, Sachin D. Experimental analysis and characterisation of chip segmentation in dry machining of Ti-6Al-4V alloy using inserts with hybrid textures. **CIRP Journal of Manufacturing Science and Technology**, v. 36, p. 213-226, jan. 2022. Disponível em: https://doi.org/10.1016/j.cirpj.2021.12.004. Acesso em: 14 jan. 2026. Acesso em: 14 jan. 2026.

SOUZA, Alex Fernandes; SOUZA, Luiz Leonardo; GAUDÊNCIO, João Henrique D.; et al. Wear classification in Ti6Al4V machining using explainable machine learning: a decision support approach. **Journal of the Brazilian Society of Mechanical Sciences and Engineering**, Cham, v. 48, art. 103, 2026. Disponível em: https://doi.org/10.1007/s40430-025-06078-8.

YADAV, Sunil Kumar; YADAV, Sanjeev Kumar Singh**.** Multi-Objective Optimization of Electrochemical Cut-off Grinding Process of Ti-6Al-4V using PCA based Grey Relational Analysis. **Materials Today: Proceedings**, v. 22, parte 4, p. 3089-3099, 2020. Disponível em: https://doi.org/10.1016/j.matpr.2020.03.445. Acesso em: 14 jan. 2026.

YU, Aihua; ZHOU, Qingjun; PAN, Yu; WAN, Fucheng; KUANG, Fan; LU, Xin**.** Hybrid clustering-enhanced interpretable machine learning for fatigue life prediction across various cyclic stages in laser powder bed fused Ti-6Al-4V alloy. **International Journal of Fatigue**, v. 198, 108995, set. 2025. Disponível em: https://doi.org/10.1016/j.ijfatigue.2025.108995. Acesso em: 14 jan. 2026.